Energy & Environmental Science

Cite this: *Energy Environ. Sci.*, 2011, **4**, 3374

www.rsc.org/ees

COMMUNICATION

Near-infrared laser-driven polymer photovoltaic devices and their biomedical applications

Jyh-Lih Wu, Fang-Chung Chen,* Ming-Kai Chuang and Kim-Shih Tan

Received 13th May 2011, Accepted 20th June 2011
DOI: 10.1039/c1ee01723c

We demonstrate near-infrared laser-driven (NIRLD) organic photovoltaic devices (OPVs), which can directly convert 980 nm light into electrical power. We attribute the NIR photovoltaic response to the long-wavelength absorption of charge transfer (CT) states. Direct excitation through CT states might open up new avenues for harvesting the long-wavelength spectrum of solar irradiation. Further, because of the high transparency of biological tissue toward 980 nm light, these NIRLD OPVs might be a promising wireless electrical source for biological nanodevices.

Organic photovoltaic devices (OPVs) are attracting increasing attention because of their low cost, flexibility, ease of processing, and abundant availability. The working principle of an OPV involves five steps: (i) exciton generation, (ii) exciton diffusion, (iii) exciton dissociation, (iv) charge transport, and (v) charge collection.[1,2] When a photon is absorbed by the photoactive layer, a bound electron/hole pair (exciton) is created. The photogenerated exciton must undergo dissociation into free carriers to contribute to the photocurrent.[3] For OPV devices, however, exciton dissociation occurs only at the donor–acceptor (D–A) interface, where an energy difference exists between the electronic levels of the involved materials, because of the relatively high binding energies of organic excitons.[1,4] Therefore, bulk heterojunction (BHJ) structures, in which a polymer (donor) and a fullerene (acceptor) form an interpenetrating network possessing a large D–A interfacial area, can be used to enhance the degree of exciton dissociation to provide higher efficiencies.[5,6] The reported power conversion efficiencies (PCEs) of OPVs based on BHJ structures have reached up to 6–8%,[7–10] rendering OPVs as promising candidates for use in next-generation solar cells.

In addition to converting solar energy into electrical power, another possible application of OPVs is to electrically drive nanodevices for biomedical treatment.[11] Because of the high transparency of biological tissues in the near-infrared (NIR) wavelength regime,[11] NIR light can be exploited directly as an energy source for *in vivo* nanorobots and biodevices. Therefore, photovoltaic devices that can efficiently convert NIR light into electricity are in high demand. Recently, Chen *et al.* reported the fabrication of 980 nm laser-driven dye-sensitized solar cells incorporating rare-earth up-converting nanophosphors.[11] The up-converted visible luminescence could be used to excite dye-sensitized TiO_2 films, leading to photovoltaic characteristics. Nevertheless, the use of phosphors complicates the device structure and the fabrication process; on the other hand, the biological non-compatibility of such devices would probably limit their practicability in realistic cases.

In this study, we developed an NIRLD OPV device based on a blend of poly(3-hexylthiophene) (P3HT) and [6,6]-phenyl-C_{61}-butyric acid methyl ester (PCBM) and systematically characterized its photovoltaic response when illuminated with 980 nm monochromatic light. Surprisingly, this OPV could be driven by a NIR laser, producing remarkable electrical power, even though the photoactive materials—the conjugated polymer and the fullerene—do not absorb

Department of Photonics and Institute of Electro-optical Engineering, National Chiao Tung University, Hsinchu, 30010, Taiwan. E-mail: fcchen@mail.nctu.edu.tw; Fax: +886-3-5735601; Tel: +886-3-5131484

Broader context

Organic photovoltaic devices (OPVs) are attracting a great deal of attention for their practical use as lightweight, flexible, low-cost, and renewable energy systems. Up to now, the most representative high-efficiency OPVs have been fabricated based on the bulk heterojunction (BHJ) concept, where a light-absorbing polymer (donor) and a soluble fullerene (acceptor) form an interpenetrating network possessing a large donor–acceptor interfacial area for efficient exciton dissociation. Meanwhile, the existence of the charge transfer (CT) states in the donor–acceptor blends, which can absorb long-wavelength photons, has been observed and investigated. Direct excitation through these CT states might open up new opportunities for utilizing the near-infrared region of solar irradiation. Based on such a unique feature, we utilized polymer/fullerene OPVs to convert 980 nm photons into electrical power. Because of the high transparency of biological tissues toward 980 nm light, our NIRLD OPVs can still produce sufficient electrical power to drive many kinds of nanodevices even when covered with a layer of porcine skin, serving as a model biological tissue. This suggests that our NIRLD OPV device can serve as a promising electrical source for nanodevices in biomedical applications.

NIR photons directly. Because 980 nm light can typically penetrate into biological tissues to a depth of several centimeters,[11] this NIRLD OPV might serve as a promising electrical source for future biomedical nanodevices. Furthermore, our study of the temperature dependence of the open-circuit voltage (V_{oc}) revealed that the maximum value [$(V_{oc})_{max}$] for this OPV, under 980 nm illumination, was governed by the energy difference between the lowest unoccupied molecular orbital (LUMO) of the acceptor and the highest occupied molecular orbital (HOMO) of the donor. These results suggest that the NIR photons were absorbed by the charge transfer (CT) states—a result of the electronic intra-gap state arising from wave function overlaps between the D and A materials.[12–16] Overall, the presented NIRLD OPV devices produced sufficient electrical output power—even after they had been covered with a layer of porcine skin, serving as a model biological tissue. Finally, the device did not require any up-converting mediate, thereby resulting in a simpler device structure and a more efficient manufacturing procedure.

Fig. 1 displays the device structure incorporating the BHJ and the chemical structures of the materials used in the active layers. The OPV device was fabricated on an indium tin oxide (ITO)-coated glass substrate. After cleaning, the ITO-coated glass was dried in an oven for at least 12 h and treated with UV ozone prior to use. The anodic buffer, poly(3,4-ethylenedioxythiophene):polystyrenesulfonate (PEDOT:PSS), was deposited on top of the ITO-coated glass through spin coating and then the sample was baked at 120 °C for 1 h. The photoactive layer, prepared from a blend of P3HT and PCBM (1 : 1, w/w) in 1,2-dichlorobenzene, was spin-coated onto the PEDOT:PSS layer. The resulting active layer was 125 nm thick. For comparison, the acceptor (PCBM) was replaced by another C_{60} derivative, indene-C_{60} bisadduct (ICBA), which possesses a higher LUMO energy level.[10,17] The wet film underwent solvent annealing in a glass Petri dish for at least 2 h.[18] Prior to thermal evaporation of the cathode, consisting of Ca (30 nm) and Al (100 nm), the active blend was thermally annealed at 110 °C for 15 min. The device area, defined through a shadow mask, was 0.12 cm^2. The completed device was encapsulated by a cover glass and sealed with a UV-curing epoxy resin prior to device characterization. The *I–V* characteristics of the devices were measured using a Keithley 2400 source-measure unit. The photocurrent response was obtained under illumination from a 150 W Thermal Oriel solar simulator (AM 1.5G) and from a 980 nm laser at various levels of power. The irradiation region of the simulated solar light covered the whole device; that of the 980 nm laser (*ca.* 3 mm^2) was smaller than the device area.

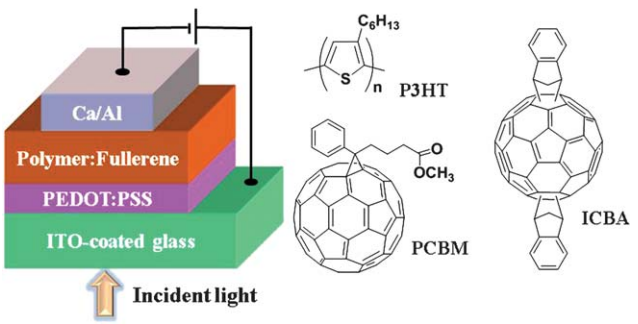

Fig. 1 Architecture of the OPV device and chemical structures of the materials used in the active layer.

Fig. 2(a) and (b) compares the current–voltage (*I–V*) characteristics of the P3HT/PCBM OPV obtained under illumination with simulated solar light (AM 1.5G) and 980 nm monochromatic light, respectively. When the device was characterized under illumination with simulated solar light [Fig. 2(a)], it exhibited photovoltaic characteristics with a value of V_{oc} of 0.59 V, a short-circuit current (I_{sc}) of 0.92 mA, and a fill factor (FF) of 0.64, resulting in a PCE of 2.87%. We attribute this relatively low PCE to the use of the relatively thin active layer (125 nm); optimal conditions typically require an active layer thickness of greater than 180 nm.[18,19] Our attention was drawn to our finding that the OPV device also exhibited a notable NIR photovoltaic response. When we illuminated the device under 980 nm monochromatic light at a power of 16.9 mW [Fig. 2(b)], the values of V_{oc}, I_{sc}, and FF were 0.43 V, 7.00 μA, and 0.70, respectively, thereby achieving a PCE of 0.0124% and a maximum output power (P_{max}) of 2.10 μW. Moreover, we calculated the external quantum efficiency (EQE) at λ_{exc} = 980 nm to be 0.0524%. The observed NIR photovoltaic response is probably associated with CT states exhibiting long-wavelength optical absorption.[14–16] Notably, the value of V_{oc} obtained from a 980 nm laser was relatively lower than that obtained under the simulated solar light. This phenomenon presumably arose from the following factors. First, the irradiation region of the 980 nm laser (*ca.* 3 mm^2) was much smaller than the device area (0.12 cm^2), causing excess dark current and, thereby, reducing the value of V_{oc}.[20] On the other hand, based on the Shockley model, where V_{oc} has a logarithmic dependence on the photocurrent,[21,22] the relatively lower value of I_{sc} obtained under 980 nm monochromatic illumination also accounted for the lower value of V_{oc} [Fig. 2(b)].

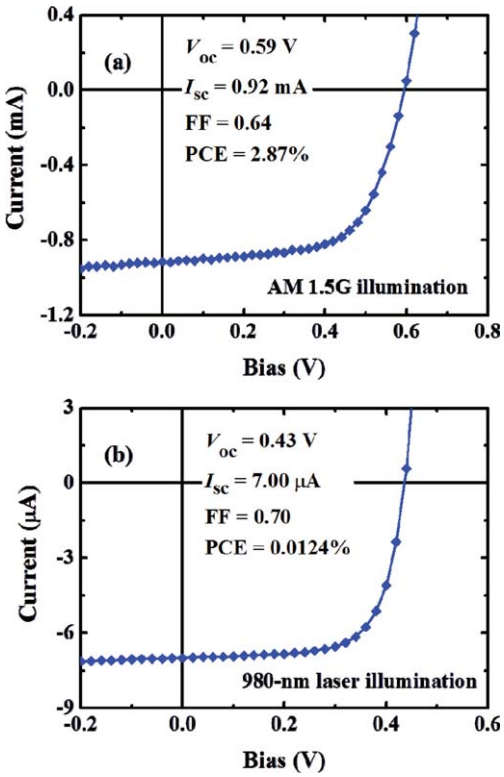

Fig. 2 *I–V* characteristics of the OPV device obtained from two different light sources: (a) simulated solar light (AM 1.5G) at 100 mW cm^{-2} and (b) 980 nm laser at a power of 16.9 mW.

We also investigated the irradiation power dependence of the photovoltaic characteristics for our NIRLD device [Fig. 3(a) and (b). The values of V_{oc} [Fig. 3(a)] and FF [Fig. 3(b)] remained relatively unchanged—from 0.43 to 0.47 V and from 0.68 to 0.71, respectively—within the studied range of laser power. On the other hand, the value of I_{sc} scaled linearly with the laser power when the laser power was less than *ca.* 55 mW [see Fig. 3(a)]. At higher laser powers, however, a deviation from the tendency occurred, presumably because of the presence of space charge and/or bimolecular recombination effects,[23] or because of photo-degradation of the device under high-intensity illumination. Correspondingly, the PCE decreased significantly upon increasing the laser power. Because the 980 nm laser intensity limit for human skin exposure is *ca.* 726 mW cm^{-2},[24] the operating laser power would have to be set at less than 21.8 mW (spot size: *ca.* 3 mm^2 in this study) if such a device were to be used in biological applications. This implies that our NIRLD OPV can still supply sufficient electrical power at lower laser power.

Previous reports have detailed the strong correlation between the value of V_{oc} and the energies of the CT states in OPVs[14,16,25]—both are governed by the band offset between the HOMO of the donor and the LUMO of the acceptor.[26,27] Meanwhile, the CT state energy also determines the value of $(V_{oc})_{max}$ in OPV devices.[28] Consequently, further investigation on the values of V_{oc}, obtained under illumination with 980 nm monochromatic light, would enable us to clarify the underlying mechanism responsible for the observed NIR photovoltaic response. Therefore, our interest was triggered to examine the temperature dependence of the values of V_{oc} to provide information allowing us to calculate the value of $(V_{oc})_{max}$.[21,22,29] In general, the value of V_{oc} of an OPV device can be expressed as[29,30]

$$V_{oc} = \frac{E_{gap}}{q} - \frac{kT}{q}\ln\left[\frac{(1-P)\gamma N_c^2}{PG}\right] \quad (1)$$

where E_{gap} is the effective band gap, P is the exciton dissociation possibility, G is the exciton generation rate, γ is the Langevin recombination constant, and N_c is the effective density of states. From eqn (1), the value of $(V_{oc})_{max}$ can be determined from the temperature dependence of V_{oc}, *i.e.*, the value of V_{oc} at a temperature of 0 K. In the case when both the organic/metal contacts are ohmic (as presented herein), the value of $(V_{oc})_{max}$ is governed by the energy difference between the LUMO of the acceptor and the HOMO of the donor.[29,31] Inevitably, the band bending effect originating from the diffusion/accumulation of charge carriers at the organic/metal interfaces leads to a reduction in the value of V_{oc}.[14,31] The degree of the voltage drop depends on the temperature and the illumination intensity;[14] typically, the deviation between the value of V_{oc}, observed at room temperature and under one sun illumination, and that of $(V_{oc})_{max}$ lies within the range of 0.3–0.5 V.[14,26,28,31] However, the value of V_{oc} reaches its maximum while the band bending effect is suppressed at a temperature of 0 K. Fig. 4(a) presents a plot of V_{oc} as a function of the device temperature for the P3HT/PCBM-based solar cell, recorded under illumination with 980 nm monochromatic light (21.63 mW). From Fig. 4(a), the value of V_{oc} decreased linearly with the increasing device temperature; extrapolation of V_{oc} to a temperature of 0 K resulted in a value of $(V_{oc})_{max}$ of 0.99 V. This value is very close to the theoretical prediction for the band offset between the HOMO of P3HT and the LUMO of PCBM of *ca.* 1.0 eV,[32,33] a factor that also determines the CT state energy.[27] Our observations suggested that CT excitons could be generated directly using 980 nm monochromatic light as the excitation source.

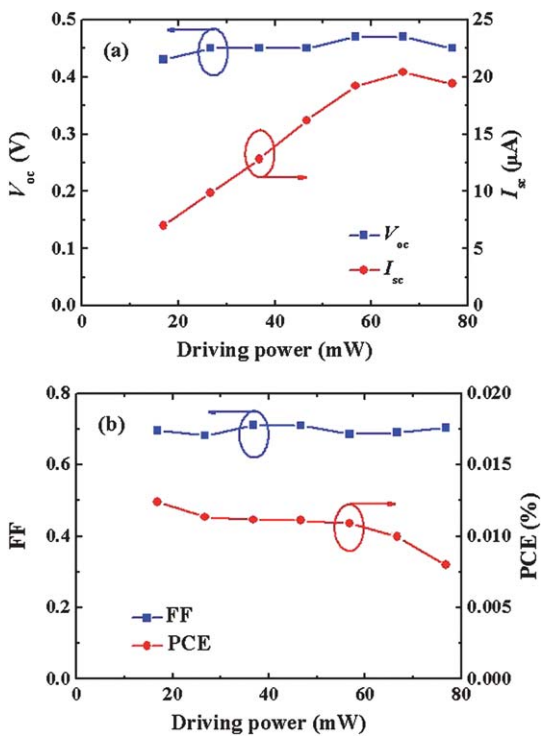

Fig. 3 Laser power dependence of the photovoltaic characteristics for the NIRLD OPV. (a) V_{oc} and I_{sc}; (b) FF and PCE.

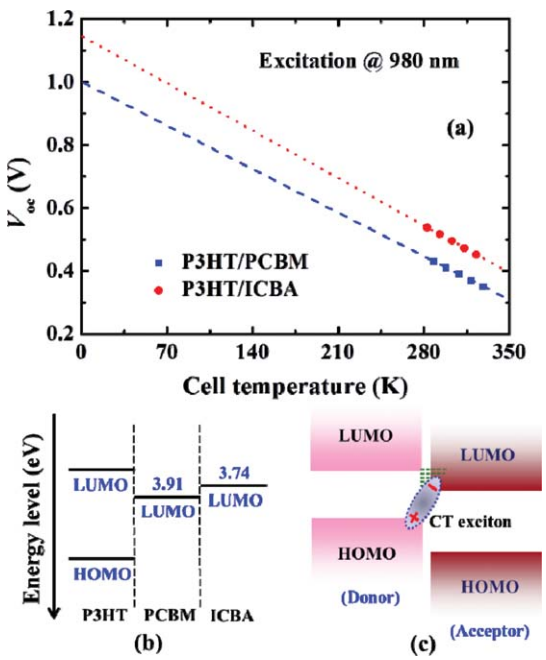

Fig. 4 (a) Plot of V_{oc} as a function of the device temperature, recorded under illumination with a 980 nm laser (power: 21.63 mW). Extrapolated values of $(V_{oc})_{max}$ for the devices based on P3HT/PCBM and P3HT/ICBA: 0.99 and 1.15 eV, respectively. (b) Energy level diagram of the active layer materials. (c) Cartoon illustration of the formation of CT excitons across the D–A interface.

To provide further evidence for this hypothesis, we determined the value of $(V_{oc})_{max}$ for a device prepared from a blend of P3HT and another fullerene derivative, ICBA (Fig. 1), in which ICBA features a LUMO energy level 0.17 eV higher than that of PCBM [Fig. 4(b)].[10,17] From Fig. 4(a), the value of $(V_{oc})_{max}$ for the P3HT/ICBA-based device was 1.15 eV—as expected, it was larger than that of the P3HT/PCBM-based device. Gratifyingly, the increased value of $(V_{oc})_{max}$ for the P3HT/ICBA-based device (0.16 V) was in an excellent agreement with the theoretical comparison (0.17 V).[10,17] This finding suggests the strong and sole dependence of the value of $(V_{oc})_{max}$ on the CT state energy, being consistent with previously proposed results.[28] Once the CT states form in a D/A blend, the CT excitons can be generated directly using below-gap excitation *via* "sub-gap absorption",[34,35] as depicted in Fig. 4(c). Therefore, we attribute the NIR photovoltaic response of the device to the long-wavelength absorption of the CT states.[14–16]

By taking advantage of the high transparency for biological tissues in the NIR region,[11] NIRLD solar cells potentially pave the way toward electrical sources for biological nanodevices. To evaluate its feasibility, we characterized the *I–V* curve of our NIRLD OPV device covered with a 3 mm-thick layer of porcine skin, which served as a model biological tissue (see Fig. 5). The power of the incident 980 nm laser was set at 21.63 mW (spot size: *ca.* 3 mm^2), taking the laser intensity limit for human skin exposure (726 mW cm^{-2}) into account. In the absence of the porcine skin, the device achieved a value of V_{oc} of 0.43 V, a value of I_{sc} of 8.56 μA, and a FF of 0.71, resulting in a PCE of 0.012% and a value of P_{max} of 2.61 μW. Note that the laser power studied here was very close to the maximum value that human skin can tolerate. After placing the porcine skin in front of the device, the device provided a value of P_{max} of 0.32 μW (V_{oc} = 0.37 V; I_{sc} = 1.28 μA; FF = 0.67; PCE = 0.00147%). This value of P_{max} might be underestimated because the rough surface of the porcine skin might have led to a higher level of light scattering. Nevertheless, this output power (P_{max} = 0.32 μW) would be sufficient to drive a biological nanodevice; the typical power requirement of which is *ca.* 10 nW.[11] Therefore, the NIRLD OPV device positioned underneath the porcine skin could, theoretically, drive several tens of nanodevices. We also note that previous results have indicated that P3HT thin films exhibited biocompatibility with living cells after appropriate surface treatment.[36] Together with excellent mechanical flexibility of OPVs,[37,38] these potential features suggest that our proposed NIRLD OPV has high potential for biological compatibility. We believe that the performance of our NIRLD OPV might be further improved though further device optimization, such as controlling the thin film morphology;[13,15,39,40] such studies are ongoing.

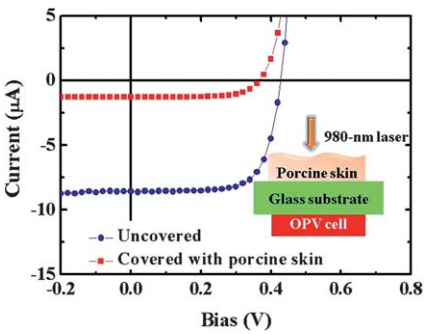

Fig. 5 *I–V* characteristics of the NIRLD OPV, uncovered and covered with a 3 mm thick layer of porcine skin. Irradiation power of the 980 nm laser: 21.63 mW (within the laser intensity limit of human skin exposure). Inset: schematic representation of the NIRLD OPV device positioned underneath the porcine skin.

In conclusion, we have realized an NIRLD OPV based on the long-wavelength CT absorption of a P3HT/PCBM blend. Measurements of $(V_{oc})_{max}$ revealed that the NIR photovoltaic response resulted from the direct excitation of the CT excitons. No up-converting mediate was required to harvest long-wavelength photons, simplifying the device structure. The high transparency of biological tissues toward 980 nm light offers the possibility of using our NIRLD OPV device as a wireless electrical source for biological nanodevices. When covered with a 3 mm thick layer of porcine skin, serving as a model biological tissue, the NIRLD OPV device still produced sufficient power to drive many nanodevices at an operating power below the safe limit. Finally, direct excitation through CT states might open up new avenues for harvesting the long-wavelength spectrum of solar irradiation to provide higher-efficiency solar cells.

Acknowledgements

We thank the National Science Council of Taiwan (NSC 99-2221-E-009-181 and NSC 100-3113-E-009-005) and the Ministry of Education of Taiwan (through the ATU program) for financial support.

Notes and references

1 P. W. M. Blom, V. D. Mihailetchi, L. J. A. Koster and D. E. Markov, *Adv. Mater.*, 2007, **19**, 1551.
2 B. Kippelen and J. L. Brédas, *Energy Environ. Sci.*, 2009, **2**, 251.
3 Y. Zhou, M. Eck and M. Krüger, *Energy Environ. Sci.*, 2010, **3**, 1851.
4 X. Y. Zhu, Q. Yang and M. Muntwiler, *Acc. Chem. Res.*, 2009, **42**, 1779.
5 N. S. Sariciftci, L. Smilowitz, A. J. Heeger and F. Wudl, *Science*, 1992, **258**, 1474.
6 G. Yu, J. Gao, J. C. Hummelen, F. Wudl and A. J. Heeger, *Science*, 1995, **270**, 1789.
7 H. Y. Chen, J. H. Hou, S. Q. Zhang, Y. Y. Liang, G. W. Yang, Y. Yang, L. P. Yu, Y. Wu and G. Li, *Nat. Photonics*, 2009, **3**, 649.
8 J. H. Hou, H. Y. Chen, S. Q. Zhang, R. I. Chen, Y. Yang, Y. Wu and G. Li, *J. Am. Chem. Soc.*, 2009, **131**, 15586.
9 Y. Y. Liang, Z. Xu, J. B. Xia, S. T. Tsai, Y. Wu, G. Li, C. Ray and L. P. Yu, *Adv. Mater.*, 2010, **22**, E135.
10 G. J. Zhao, Y. J. He and Y. F. Li, *Adv. Mater.*, 2010, **22**, 4355.
11 Z. G. Chen, L. S. Zhang, Y. G. Sun, J. Q. Hu and D. Y. Wang, *Adv. Funct. Mater.*, 2009, **19**, 3815.
12 M. Hallermann, S. Haneder and E. Da Como, *Appl. Phys. Lett.*, 2008, **93**, 053307.
13 M. Hallermann, I. Kriegel, E. Da Como, J. M. Berger, E. von Hauff and J. Feldmann, *Adv. Funct. Mater.*, 2009, **19**, 3662.
14 K. Vandewal, A. Gadisa, W. D. Oosterbaan, S. Bertho, F. Banishoeib, I. Van Severen, L. Lutsen, T. J. Cleij, D. Vanderzande and J. V. Manca, *Adv. Funct. Mater.*, 2008, **18**, 2064.
15 C. M. Yang, P. Y. Tsai, S. F. Horng, K. C. Lee, S. R. Tzeng, H. F. Meng, J. T. Shy and C. F. Shu, *Appl. Phys. Lett.*, 2008, **92**, 083504.
16 K. Vandewal, K. Tvingstedt, A. Gadisa, O. Inganäs and J. V. Manca, *Nat. Mater.*, 2009, **8**, 904.
17 Y. J. He, H. Y. Chen, J. H. Hou and Y. F. Li, *J. Am. Chem. Soc.*, 2010, **132**, 5532.
18 F. C. Chen, C. J. Ko, J. L. Wu and W. C. Chen, *Sol. Energy Mater. Sol. Cells*, 2010, **94**, 2426.
19 F. C. Chen, J. L. Wu and Y. Hung, *Appl. Phys. Lett.*, 2010, **96**, 193304.
20 J. S. Huang, G. Li and Y. Yang, *Adv. Mater.*, 2008, **20**, 415.

21 E. A. Katz, D. Faiman, S. M. Tuladhar, J. M. Kroon, M. M. Wienk, T. Fromherz, F. Padinger, C. J. Brabec and N. S. Sariciftci, *J. Appl. Phys.*, 2001, **90**, 5343.
22 I. Riedel, E. von Hauff, H. Parisi, N. Martin, F. Giacalone and V. Dyakonov, *Adv. Funct. Mater.*, 2005, **15**, 1979.
23 R. A. Marsh, C. R. McNeill, A. Abrusci, A. R. Campbell and R. H. Friend, *Nano Lett.*, 2008, **8**, 1393.
24 American National Standard for Safe Use of Lasers, *ANSI Z136. 1–2000*, American National Standard Institute, Orlando, FL, 2000.
25 M. Hallermann, E. Da Como, J. Feldmann, M. Izquierdo, S. Filippone, N. Martin, S. Juchter and E. von Hauff, *Appl. Phys. Lett.*, 2010, **97**, 023301.
26 M. C. Scharber, D. Wuhlbacher, M. Koppe, P. Denk, C. Waldauf, A. J. Heeger and C. L. Brabec, *Adv. Mater.*, 2006, **18**, 789.
27 J. J. Benson-Smith, L. Goris, K. Vandewal, K. Haenen, J. V. Manca, D. Vanderzande, D. D. C. Bradley and J. Nelson, *Adv. Funct. Mater.*, 2007, **17**, 451.
28 D. Veldman, S. C. J. Meskers and R. A. J. Janssen, *Adv. Funct. Mater.*, 2009, **19**, 1939.
29 F. C. Chen, J. L. Wu, S. S. Yang, K. H. Hsieh and W. C. Chen, *J. Appl. Phys.*, 2008, **103**, 103721.
30 L. J. A. Koster, V. D. Mihailetchi, R. Ramaker and P. W. M. Blom, *Appl. Phys. Lett.*, 2005, **86**, 123509.
31 V. D. Mihailetchi, P. W. M. Blom, J. C. Hummelen and M. T. Rispens, *J. Appl. Phys.*, 2003, **94**, 6849.
32 L. J. A. Koster, V. D. Mihailetchi and P. W. M. Blom, *Appl. Phys. Lett.*, 2006, **88**, 093511.
33 M. D. Irwin, B. Buchholz, A. W. Hains, R. P. H. Chang and T. J. Marks, *Proc. Natl. Acad. Sci. U. S. A.*, 2008, **105**, 2783.
34 T. Drori, C. X. Sheng, A. Ndobe, S. Singh, J. Holt and Z. V. Vardeny, *Phys. Rev. Lett.*, 2008, **101**, 037401.
35 J. Lee, K. Vandewal, S. R. Yost, M. E. Bahlke, L. Goris, M. A. Baldo, J. V. Manca and T. Van Voorhis, *J. Am. Chem. Soc.*, 2010, **132**, 11878.
36 G. Scarpa, A. L. Idzko, S. Gotz and S. Thalhammer, *Macromol. Biosci.*, 2010, **10**, 378.
37 S. I. Na, S. S. Kim, J. Jo and D. Y. Kim, *Adv. Mater.*, 2008, **20**, 4061.
38 F. C. Chen, J. L. Wu, C. L. Lee, W. C. Huang, H. M. P. Chen and W. C. Chen, *IEEE Electron Device Lett.*, 2009, **30**, 727.
39 L. Goris, A. Poruba, L. Hod'ákova, M. Vaněček, K. Haenen, M. Nesládek, P. Wagner, D. Vanderzande, L. De Schepper and J. V. Manca, *Appl. Phys. Lett.*, 2006, **88**, 502113.
40 D. H. Wang, J. K. Kim, O. O. Park and J. H. Park, *Energy Environ. Sci.*, 2011, **4**, 1434.

